Applied Catalysis B: Environmental 130–131 (2013) 99–105

Contents lists available at SciVerse ScienceDirect

Applied Catalysis B: Environmental

journal homepage: www.elsevier.com/locate/apcatb

Development of a doped titania immobilised thin film multi tubular photoreactor

Morgan Adams*, Nathan Skillen, Cathy McCullagh, Peter K.J. Robertson

IDEAS, Institute for Innovation, Design and Sustainability Research, CREE, Centre for Research in Energy and the Environment, The Robert Gordon University, School of Engineering, Aberdeen AB10 1FR, UK

ARTICLE INFO

Article history:
Received 27 February 2012
Received in revised form
20 September 2012
Accepted 14 October 2012
Available online 23 October 2012

Keywords:
Photocatalysis
Thin film
Titanium dioxide (TiO_2)
Lanthanides
Surface area

ABSTRACT

This paper describes a novel doped titania immobilised thin film multi tubular photoreactor which has been developed for use with liquid, vapour or gas phase media. In designing photocatalytic reactors measuring active surface area of photocatalyst within the unit is one of the critical design parameters. This dictate greatly limits the applicability of any semi-conductor photocatalyst in industrial applications, as a large surface area equates to a powder catalyst. This demonstration of a thin film coating, doped with a rare earth element, novel photoreactor design produces a photocatalytic degradation of a model pollutant (methyl orange) which displayed a comparable degradation achieved with P25 TiO_2. The use of lanthanide doping is reported here in the titania sol gel as it is thought to increase the electron hole separation therefore widening the potential useful wavelengths within the electromagnetic spectrum. Increasing doping from 0.5% to 1.0% increased photocatalytic degradation by ~17% under visible irradiation. A linear relationship has been seen between increasing reactor volume and degradation which would not normally be observed in a typical suspended reactor system.

1. Introduction

Semiconductor photocatalysis is an important area of research and is an ever growing industrial tool which is applicable to a wide range of fields. Semiconductor photocatalysis has grown significantly in the last three decades, and has been applied to a diverse array of environmental problems including air [1], potable and wastewater treatment [2], as well as photo-splitting of water to produce hydrogen gas [3–5], nitrogen fixation [6–8], and microbe destruction [9].

While the application of photocatalysis has become diverse there remain 3 key areas that are critical in developing an effective treatment process: light source, reaction vessel and photocatalyst. Recent literature has shown a movement from utilising ultra-violet (UV) to visible light driven photocatalysis with a view towards industrial applications [10–12]. TiO_2 is restricted to UV light due to its band gap energy of ~3.2 eV. In an attempt to overcome this limitation metal doping has been successfully utilised to move the band gap of TiO_2 into the visible region. Lanthanide doping has been reported in the literature, primarily in conjunction with TiO_2 to produce nano-composites [13–15]. The addition of lanthanide ions to TiO_2 is thought to increase the electron hole separation [16,17].

In an increasingly energy efficient world, high power and energy demanding light sources are becoming less suitable. Much of the literature has demonstrated experimental designs which utilise ≥500 W medium/high pressure lamps [18–21]. These lamps are less practical for industrial applications due to their fragility, high energy consumption and are not essential for high efficiency photocatalysis. This raises concern over the true photocatalytic activity of a catalyst when used in conjunction with high powered lamps.

The use of TiO_2 powders, such as Degussa P25, is also restricted in relation to downstream processing, as separation can be problematic in industries such as water purification. The nanoparticulate size of P25 results in filtration becoming a labour intensive and expensive procedure. Methods have been proposed to overcome these obstacles including the use of the pelletised form of TiO_2 [22–24] and immobilising catalysts onto a solid support [25,26]. Pelletised TiO_2 has been known to 'crumble' due to mechanical abrasion, which again raises filtration problems. The immobilisation of catalysts presents an alternative process for deployment of photocatalysts that eliminates the requirement to separate the photocatalyst from the treated water. A number of different coating methods have been reported [27–30] on a range of different solid supports including steel, titanium, activated carbon, zeolites, glass, quartz, glass fibres, optical fibres and silica [22,31–36].

In order to demonstrate the viability of semiconductor photocatalysis for industrial applications, reactor design is an equally critical factor. Scaling up photocatalytic reactors is however, a complex process with many factors requiring consideration to yield a technically and economically efficient process. These factors include distribution of target species and photocatalyst, mass transfer, reaction kinetics and irradiation characteristics. The issue

* Corresponding author. Tel.: +44 1224 262840; fax: +44 1224 262444.
E-mail address: m.adams1@rgu.ac.uk (M. Adams).

0926-3373/$ – see front matter © 2012 Elsevier B.V. All rights reserved.
http://dx.doi.org/10.1016/j.apcatb.2012.10.008

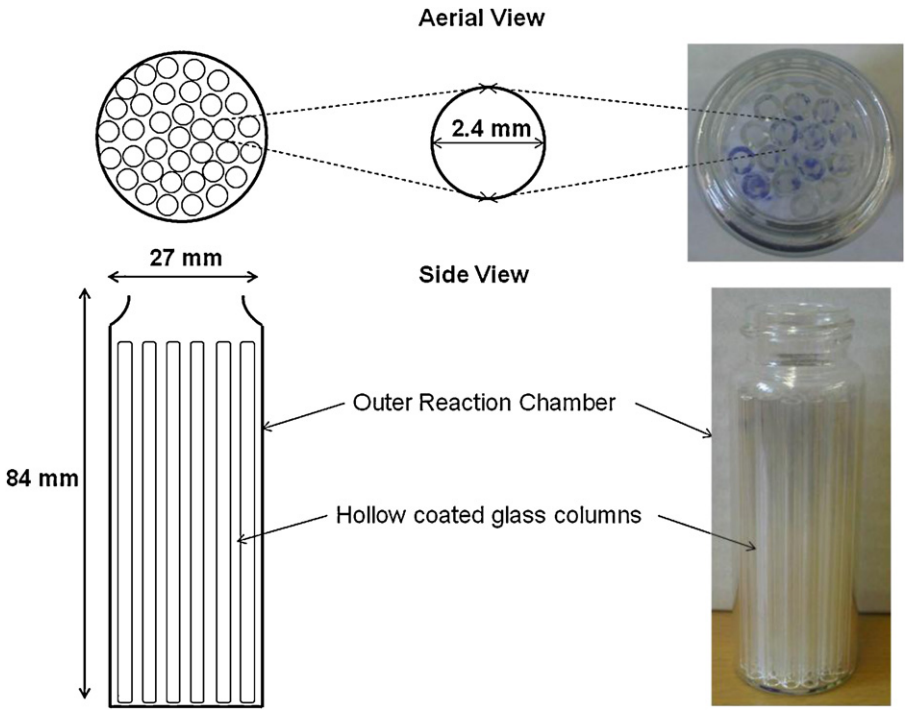

Fig. 1. Arrangement of multi tubular photoreactor.

of effective photocatalyst illumination is particularly important as this essentially determines the amount of fluid or gas that may be treated per effective unit area of deployed photocatalyst.

Photocatalytic activity can be significantly affected by the surface area of a catalyst. A number of investigations have been reported which aim to increase photocatalytic efficiency by increasing surface area. Surface areas of photocatalysts in the range of 27.5 m^2/g through to 400 m^2/g have been reported [37,38]. The literature generally states that increasing surface area will improve photocatalytic activity as an increased number of sites for photocatalytic reactions will be present. This was the focus of an investigation by Amano et al. [39] where CO_2 evolution from acetaldehyde decomposition increased with an increasing specific surface area from 10 to ~33 m^2/g. Furthermore, investigations have attempted to increase the already high surface area of TiO_2 (50 m^2/g) in an attempt to improve photocatalytic transformations. Phonthammachai et al. produced TiO_2 with a high surface area of 163 m^2/g for inclusion into a membrane for the degradation of 4-nitrophenol [40].

This paper reports the development of a novel thin film multi tubular photoreactor incorporating a lanthanide doped titania sol gel coating. The performance of the reactor has been evaluated through monitoring the degradation of methyl orange (MO) as a model dye pollutant. MO has been chosen as the target for degradation as it is a more stable dye molecule than methylene blue. This makes MO more difficult to break down and therefore more resistant to photobleaching. The application of low powered (36 W) visible and UV lamps with a view to large scale industrial applications were examined. As a means of catalyst platform appraisal, experiments were conducted with titania sol gel coated silica beads and Degussa P25. Furthermore, experiments were conducted to determine if a linear relationship exists in the scaling up process of the coated glass columns. This investigation aimed to demonstrate that a significantly large surface area is not essential to achieve efficient photocatalytic activity, which in turn can allow for more practical photoreactor developments for industrial applications.

2. Experimental

2.1. Titania sol–gel

The sol–gel formulations were produced following a modified method by Mills et al. [41]. 4.65 g (4.43 mL) of glacial acetic acid (Sigma–Aldrich) was added to 20 mL of titanium isopropoxide (Sigma–Aldrich). To this solution 120 mL of 0.1 mol L^{-1} nitric acid (Fisher Scientific) was added before heating the mixture at 80 °C for 8 h in a water bath. The resulting opaque solution was then filtered through a 0.45 μm filter (Whatman) to remove any aggregated particles.

2.1.1. Doped titania sol–gel

To produce the doped titania films, $Nd(NO_3)_3{\cdot}6H_2O$ (Fisher Scientific), was dissolved in the 120 mL of 0.1 mol L^{-1} nitric acid before adding the solution to the titanium isopropoxide and acetic acid. Two concentrations of 0.5 wt% (0.6 g) and 1 wt% (1.6 g) were examined. The sol was completed by heating in a water bath as detailed in Section 2.1.

2.2. Coated silica particles

Coated silica particles were produced by saturating a beaker of 50–100 μm particles with the titania sol. The coated particles were then transferred to a clean flat surface where they were spread thinly and allowed to dry at room temperature before calcination at 450 °C for 30 min. The 450 °C heat treatment results in a 100% anatase titania coating.

The coated and uncoated silica particles were analysed under SEM (Leo S430) to determine the quality of coating and also to perform EDAX analysis to determine elemental distribution.

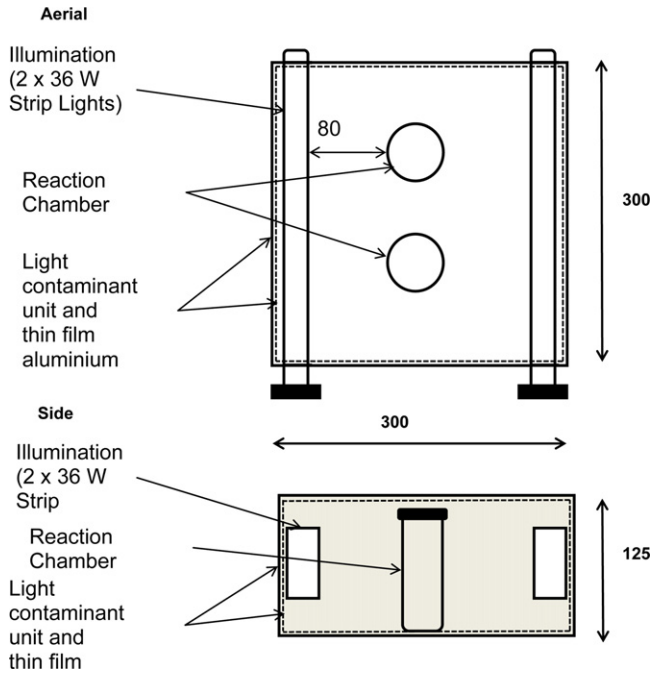

Fig. 2. Configuration of illumination box.

2.3. Multi tubular photoreactor

The multi tubular photoreactors were produced by dip coating glass tubes in the titania sol gel solution. As reported by Mills et al. [41], this traditional sol–gel film produces a coating typically around 50 nm thick. The glass tubes (Fisher Scientific) were cut into 65 mm lengths, prior to coating. These tubes were allowed to dry at room temperature before being calcined in a high temperature chamber furnace (Carbolite, UK) at 450 °C for 30 min producing an anatase coating?

The reactor vessel (Supelco, 27181), was coated on the inside with the sol gel solution and allowed to dry at room temperature before calcination at 450 °C for 30 min.

Thirty-two glass tubes were placed into the glass reactor vessel producing the unit (Fig. 1).

2.4. Experimental setup

Reaction vessels were placed in a light containment reactor which was lined with thin film aluminium and illuminated by two 36 W non-integrated compact fluorescent lamps. A range of visible and UV spectral output lamps were utilised (Fig. 2). The light containment reactor was capable of running two reaction vessels simultaneously per experiment. To maintain directly comparable parameters both the P25 and coated bead experiments were performed using the same clean glass vessels (Supelco, 27181) used for the multi tubular reactor.

During the experiments with the silica coated beads and P25 agitation of the reaction mixture was achieved by magnetic plates and stirrers. There was no agitation during experiments with the coated glass columns.

Each experiment was allowed an equilibrium time of 20 min in the dark prior to illumination for 90 min. Samples (1 mL) were taken, by syringe extraction, before and after the equilibrium period to allow the dark absorbance to be calculated. During the 90 min illumination period samples were taken every 30 min in triplicate. In addition to triplicate samples, experiments were also run in triplicate. A syringe filter (0.45 μm) was utilised to filter samples during P25 experiments. No filtration was required for the silica coated beads and immobilised coated glass columns. Analysis of samples was done by UV–vis spectrometry, monitoring absorbance of MO at 462 nm. Absorbance readings were normalised to 1.

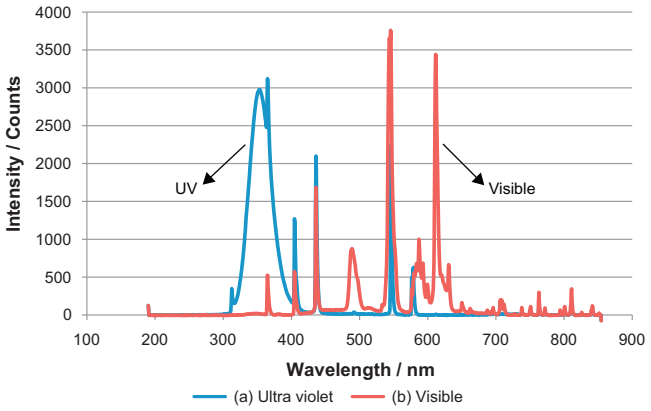

Fig. 3. Emission spectrum for UV and visible lamps.

2.4.1. Illumination sources

The two different illumination lamps used were spectrally analysed using a Stellarnet EPP2000 Spectrometer to determine their exact emissions. Fig. 3(a) shows the emission spectra of the Philips CLEO PL-L UV lamp (blue plot), which displays a large UV peak at 350 nm and a sharp shoulder peak at 365 nm. The other visible emissions can be seen at 404, 436, 546 and 578 nm.

Fig. 3(b) shows the emission spectra of the General Electric Biax L 830 (red plot) fluorescent tube which displays a single ultra violet emission of 365 nm with the remaining strong emissions in the visible region, 404, 486, 543, 587, 611 being the predominant wavelengths.

3. Results and discussion

3.1. SEM/EDAX of coated and uncoated silica particles

The SEM image, Fig. 4(a) shows uncoated silica particles exhibiting a smooth textured surface. Fig. 4(b) shows titania sol–gel coated silica particles which display a textured “cratered” and in parts slightly fracture surface. The surface effects observed are due to variation in sol gel thickness, drying and proximity of particles during furnace annealing. The majority of particles exhibit a good surface-coating interface. The thicker areas of coating tend to be more fragile and do not bond as well to the surface; improvements to the process of manufacture will eliminate the surface fracturing. Earlier studies have seen that multiple coatings of the same sol material do not increase photocatalytic activity, therefore whether a coating is thick or thin will not influence the overall efficiency of the coating.

The energy dispersive X-ray (EDAX) analysis of the uncoated and coated particles is shown in Figs. 5 and 6. As expected the uncoated silica particle produces an EDAX spectrum of a typical silica glass composition. The coated particle displays the same silica glass composition with the addition of Ti which comes from the titania sol gel coating.

Fig. 6 shows elemental evidence of the neodymium doping within the titania coating. This confirmation proves the neodymium to be an integral part of the titania matrix as it has not been washed out during filtration (0.1 mol L^{-1} nitric acid, absolute ethanol and distilled water).

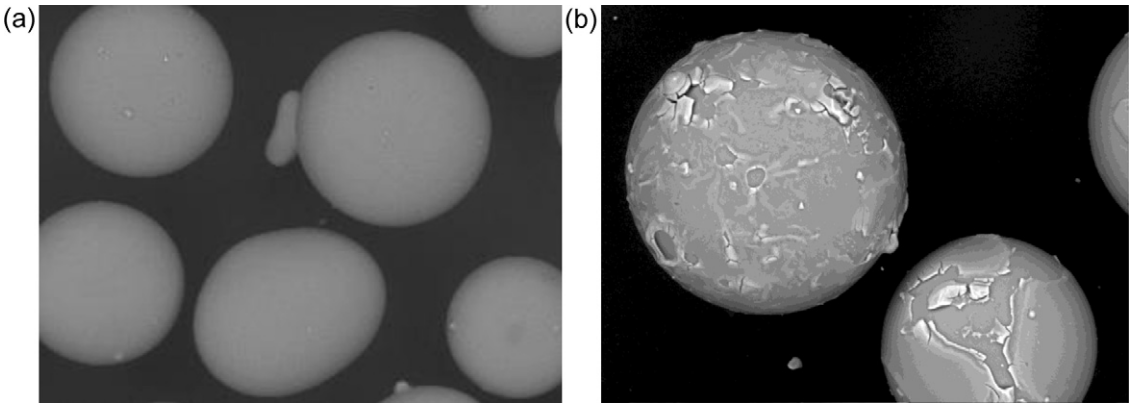

Fig. 4. (a) Uncoated silica particles and (b) titania coated silica particles.

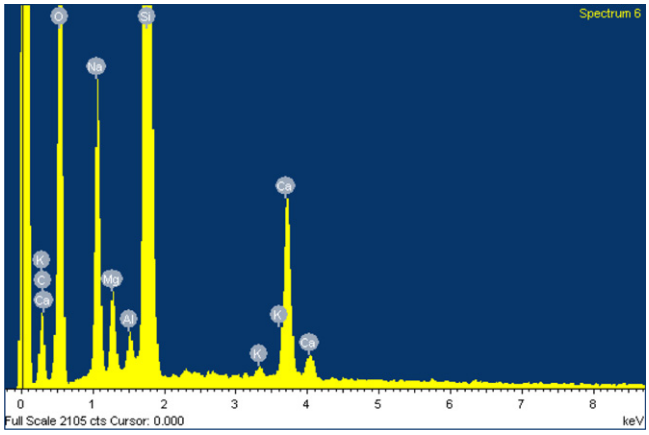

Fig. 5. EDAX spectrum of undoped silica particles.

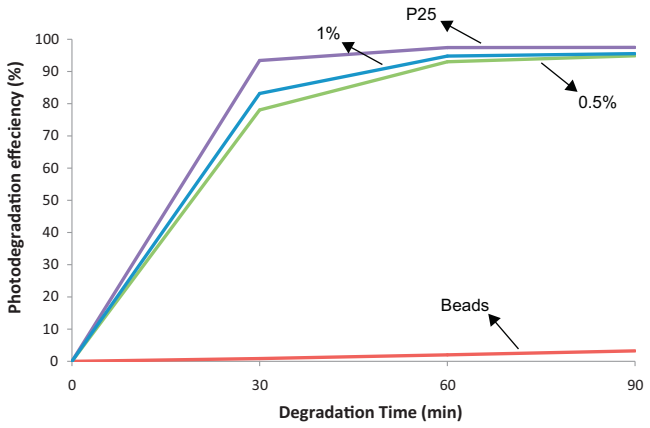

Fig. 7. Methyl orange degradation by P25 TiO_2 (purple), coated silica beads (red), coated glass tubes with 0.5% doping (green) and 1% doping (blue) – 72 W UV illumination. (For interpretation of the references to colour in this figure legend, the reader is referred to the web version of the article.)

3.2. MO degradation (UV irradiation)

Fig. 7 shows the plots for methyl orange degradation by P25, coated silica beads and coated glass tubes. The controls showed no discernible variation throughout the duration of the experiment for any catalyst platform. Under pure UV conditions 10.3% methyl orange degradation was recorded while under visible conditions 1.4% was recorded. The maximum level of dark absorbance recorded was with P25 at 5.2% which was expected due to the porous nature of the catalyst. Based upon these control result all other photodegradation observed can be attributed to photocatalytic degradation.

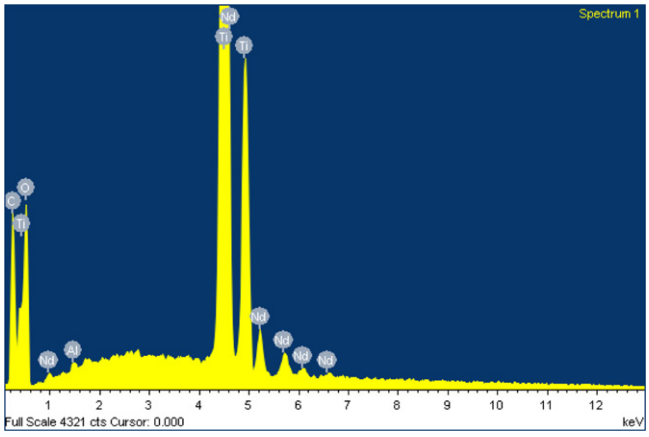

Fig. 6. EDAX spectrum of neodymium doped silica particles.

The first photocatalyst examined was P25 TiO_2, which had a surface area of ~60 m^2/g. A 97% degradation of methyl orange was achieved under UV irradiation for this material.

The second photocatalyst examined was the titania sol–gel coated silica beads, the calculated surface area of coated particles is ~0.024 m^2/g.

The final photocatalyst examined was the thin film doped titania sol gel coated tubes with a calculated surface area of ~0.04 m^2/g. Degradation of 95% for the coated tubes with a 1% doping under UV irradiation was observed.

It can be seen from the performance of the photocatalysts that the degradation of MO in the reactor was similar to the result when Deg P25 was employed, Fig. 7. In addition to a comparable overall degradation, similarities can be seen in the nature in which degradation occurs. Both the TFMCP and P25 suspended system showed a significant reduction in MO absorbance within the initial stage of illumination. After 30 min illumination 78% and 93% degradation was observed for the reactor and P25 respectively. Conventional theory shows that the higher the surface area, the greater the photocatalytic activity. Recent research has shown [39] the relationship between photocatalytic activity and CO_2 reduction follows a linear path. The linear nature of CO_2 reduction is such within static reactor configuration. If this were applied to this work it would be expected that in relation to P25 TiO_2 at 60 m^2/g, coated beads would produce a degradation of 0.04% and coated tubes would produce a degradation of 0.06% using the same experimental parameters.

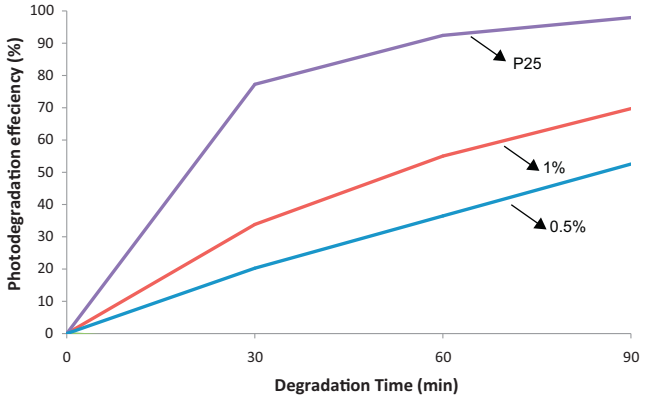

Fig. 8. Methyl orange degradation by P25 TiO_2 (purple), coated glass tubes with 0.5% doping (blue) and 1% doping (red) – 72 W visible illumination. (For interpretation of the references to colour in this figure legend, the reader is referred to the web version of the article.)

This is not the case, it was shown here that indeed the coated particles with a surface area of 0.24 m^2/g did not produce any notable degradation; this is possibly due to the particle density causing the solution to become turbid. For optimum photocatalytic activity low level turbidity is required for interaction between active surface and target [42]. In the case of the coated tubes with a surface area of 0.04 m^2/g, a degradation of 95% was achieved, which compared to that achieved with P25 materials.

3.3. MO degradation (visible irradiation)

The sol–gel coated silica beads and coated tubes were doped with the lanthanide neodymium which acts as a chelate, absorbing a broader range of wavelengths and transferring the energy to TiO_2. The addition of the dopant does not affect the intrinsic properties of the TiO_2 which still retains its UV absorbance. As was shown in Fig. 3(b), the visible lamp spectra does display a small emission peak in the UV region at 365 nm. This discrete emission peak is 16.8% of the equivalent emission spectra for the UV lamp Fig. 3(a). The following results show the effect this minor discrete emission had by the photocatalytic performance of P25.

Fig. 8 shows the plots for methyl orange degradation by P25 and coated glass tubes. The coated silica beads showed no MO degradation under the visible light conditions and are not shown in Fig. 8. As previously stated control experiments showed no discernible variation throughout the duration of the experiment for any catalyst platform.

As with the UV illumination, the first photocatalyst examined under visible irradiation, peak emissions 543 and 612 nm, was P25 TiO_2. MO degradation of 98% in the presence of Deg P25 TiO_2 under visible light irradiation was observed.

The controls for the titania sol gel tubes showed no discernible variation throughout the duration of the experiment. A degradation of 53% was achieved for the coated tubes with a 0.5% doping under visible light irradiation.

This experiment was repeated with 1.0% doping, the controls again show no discernable variation throughout the duration of the experiment. The observed degradation for the coated tubes under visible irradiation was 70%. This is a ~17% improvement over the 0.5% doped sample and shows the improved absorbance of increasing the level of dopant. The exact same reactor configuration was employed, therefore any variation of methyl orange degradation is purely due to the catalyst and no other factor.

It can be seen from the performance of the photocatalysts that the coated tubes had a slower degradation rate of MO compared to that achieved with a P25 photocatalyst. Interestingly a comparable level of degradation was achieved with P25 under visible light to UV light. This is probably due to the fact that the visible lamps emit a small amount of ultraband gap UV light which is sufficient to activate the P25 material.

The sample processing of the coated glass column reactor, following photocatalysis, was minimal in comparison to the time consuming, expensive and unreliable sample processing required with P25. Prior to analysis of the P25 treated samples filtration was required by syringe filtration; however, this method cannot provide 100% separation due to the colloidal-like suspension created by P25. This was shown by the variation observed between standard deviation of replicates, 0.0673. This level of variation was not observed in the experimental data for experiments conducted with the coated glass tubes, standard deviation of 0.0157. Furthermore when comparing the catalyst platforms, the coated silica beads (3%) showed minimal absorbance reduction suggesting no photocatalytic activity. Filtration of the silica beads was not required as they were large enough in size to fall out of suspension when agitation was stopped.

3.4. Illuminated surface area

Illuminated surface area is a controlling factor in photocatalysis and can significantly alter the rate of a reaction. The illuminated surface area of immobilised catalysts is often overlooked as powder provides a greater surface area for catalytic activity. However, immobilised reactor configurations which utilise the full catalyst

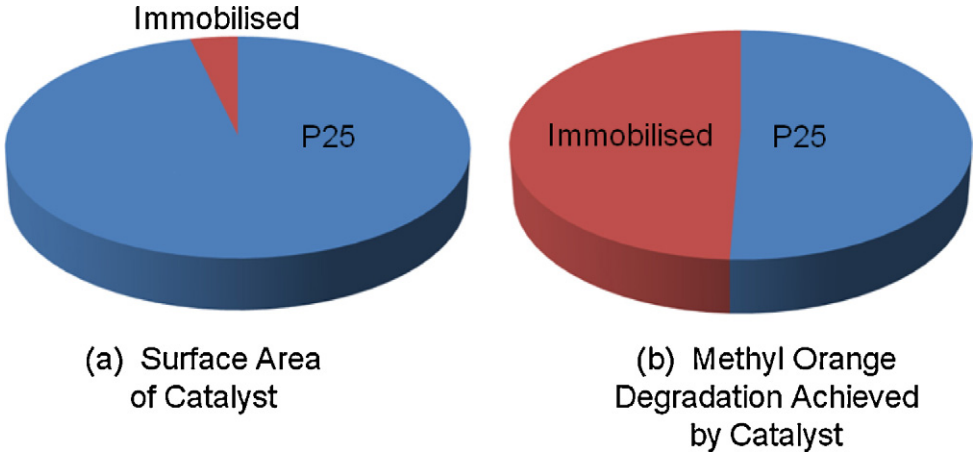

Fig. 9. Comparison of methyl orange degradation and catalyst surface area.

Table 1
Linearity of multi tubular reactor degradation rates, volume and tube number.

Reactor	Reactor volume (mL)	Number of tubes and length (mm)	Degradation at 30 min (%)	Degradation at 90 min (%)
1	20	32 × 65	78.0	94.97
2	120	61 × 200	53.88	91.78
3	250	92 × 260	75.87	91.62

coating and reduce mass transport limitations, can be highly photocatalytically active. To achieve photocatalytic efficiency in an immobilised system mass transport limitations can be reduced via close contact of catalyst and pollutant or via the agitation of the model pollutant. The thin film reactor in this investigation showed mass transport limitations can be reduced by the use of closely packed coated columns. The configuration ensures the model pollutant is constantly in close contact with a coated surface. This increases the ease of reaction between catalyst and pollutant. Fig. 9 shows the level of degradation achieved by P25 (97%) and the thin film reactor (95%) under UV light and the calculated surface area. Despite a significantly reduced surface area, in comparison to the suspended system, the immobilised catalyst performed within ~3% of the P25 suspended system. For industrial applications the TFMCP can be considered to have outperformed the suspended system as no agitation or downstream processing of samples was required which reduced the overall energy consumption, cost and time frame of the reaction.

4. Linearity of multi tubular scale up

To examine whether there was a linear relationship between volume of target media and number of tubes, two larger multi tubular photoreactors were created. From experience it was already known the issues related to increased catalyst loading, volume and energy required for agitation [22,23,43–45]. Firstly a 200 mm tube reactor (2) was created using a 250 mL measuring cylinder as the reactor vessel, secondly 260 mm tube reactor (3) was created using a 350 mL hydrometer jar as a reactor vessel, due to the large size it was not possible to coat the inside of these vessels. The 260 mm tube size was the maximum permissible tube which could be processed in the furnace.

The results from these initial experiments into scale up are shown in Table 1, which displays the number of coated tubes, tube length, reactor volume, percentage degradation at 30 min and final percentage degradation at 90 min.

5. Conclusion

It can be seen from the performance of the photocatalysts that the coated tubes produced a degradation rate similar to that of a powder catalyst under UV irradiation and 70% degradation under visible irradiation. The use of lanthanide doping has been investigated here in the titania sol gel as it is believed to enhance the electron hole separation and also to widen the absorption potential of a coating into the visible region. This was shown to occur with 1.0% doping and the observed 20% improvement over the 0.5% doped sample.

The immobilised reactor configurations reported here have demonstrated the utilisation of the full catalyst coating and therefore reduced mass transport limitations as the catalyst and dye are in constant proximity. The application of a powder catalyst in any reactor design generates sample handling issues, an inability to accurately monitor online degradation, the need to filter processed effluent streams, and the possibility of introducing "super fine" TiO_2 particles to a water course. This immobilised film unit addresses these limitations. Also the environmental impact of increased energy consumption to run a suspended powder reactor unit increases the carbon footprint, as powder is required to be separated from the model pollutant. These limitations are removed completely by the development of thin film photoreactors. There is no limitation on sample monitoring, risk of suspended material discharge or unnecessary power wastage. With increased capacity it would be more than possible to compete with existing industrial scale photoreactors. This may be achieved through application of this modular design.

This work has demonstrated the potential to develop thin film coatings, when combined with intelligent reactor configuration, allowing a photocatalytic process comparable to that of a powdered catalyst.

Acknowledgements

The authors wish to thank the Engineering and Physical Sciences Research Council for funding project EP/H004130/1, titled International Collaboration in Chemistry Enhancing Direct Photoelectrochemical Conversion of CO_2.

Morgan Adams wishes to thank EPSRC for funding his postdoctoral post and Nathan Skillen wishes to thank EPSRC for funding his PhD research. The authors would also like to thank the Scottish Funding Council who funded C. McCullagh's lectureship through the Northern Research Partnership's research pooling initiative in engineering.

References

[1] P. Yaron, Applied Catalysis B: Environmental 99 (2010) 448–460.
[2] S. Malato, P. Fernández-Ibáñez, M.I. Maldonado, J. Blanco, W. Gernjak, Catalysis Today 147 (2009) 1–59.
[3] A. Fujishima, K. Honda, Nature 238 (1972) 37–38.
[4] K.E. Karakitsou, X.E. Verykios, Journal of Physical Chemistry 97 (1993) 1184–1189.
[5] Suzuki, in: F. Ollis, H. David, Al-Ekhabi (Eds.), Photocatalytic Purification and Treatment of Water and Air, Elsevier, 1993, p. 421.
[6] M.M. Taqui Khan, N. Nageswara Rao, Journal of Photochemistry and Photobiology A: Chemistry 56 (1991) 101–111.
[7] M. Schiavello, Electrochimica Acta 38 (1993) 11–14.
[8] M.M.T. Khan, D. Chatterjee, M. Krishnaratnam, M. Bala, Journal of Molecular Catalysis 72 (1992) 13–18.
[9] C. McCullagh, J. Robertson, D. Bahnemann, P. Robertson, Research on Chemical Intermediates 33 (2007) 359–375.
[10] H. Sun, S. Wang, H.M. Ang, M.O. Tade, Q. Li, Chemical Engineering Journal 162 (2010) 437–447.
[11] W. Su, J. Chen, L. Wu, X. Wang, X. Wang, X. Fu, Applied Catalysis B: Environmental 77 (2008) 264–271.
[12] Q. Chen, D. Jiang, W. Shi, D. Wu, Y. Xu, Applied Surface Science 255 (2009) 7918–7924.
[13] X. Quan, Q. Zhao, H. Tan, X. Sang, F. Wang, Y. Dai, Materials Chemistry and Physics 114 (2009) 90–98.
[14] Y. Zhang, H. Zhang, Y. Xu, Y. Wang, Journal of Solid State Chemistry 177 (2004) 3490–3498.
[15] J.-w. Shi, J.-t. Zheng, P. Wu, Journal of Hazardous Materials 161 (2009) 416–422.
[16] Q. Xiao, Z. Si, J. Zhang, C. Xiao, Z. Yu, G. Qiu, Journal of Materials Science 42 (2007) 9194–9199.
[17] F.B. Li, X.Z. Li, C.H. Ao, S.C. Lee, M.F. Hou, Chemosphere 59 (2005) 787–800.
[18] H.-Y. Shu, M.-C. Chang, Journal of Hazardous Materials 125 (2005) 244–251.
[19] M.d.l.M. Ballari, O.M. Alfano, A.E. Cassano, Chemical Engineering Science 65 (2010) 4931–4942.
[20] M. Sharma, T. Jain, S. Singh, O.P. Pandey, Solar Energy 86 (2012) 626–633.
[21] S.-J. Kim, H.-G. Lee, S.-J. Kim, J.-K. Lee, E.G. Lee, Applied Catalysis A: General 242 (2003) 89–99.
[22] M. Adams, I. Campbell, P.K.J. Robertson, International Journal of Photoenergy 2008 (2008) 7.

[23] C. McCullagh, P.K.J. Robertson, M. Adams, P.M. Pollard, A. Mohammed, Journal of Photochemistry and Photobiology A: Chemistry 211 (2010) 42–46.
[24] N. Bouazza, M.A. Lillo-Ródenas, A. Linares-Solano, Applied Catalysis B: Environmental 77 (2008) 284–293.
[25] N.M. Mahmoodi, M. Arami, Journal of Photochemistry and Photobiology B: Biology 94 (2009) 20–24.
[26] H.F. Lin, K.T. Valsaraj, Journal of Hazardous Materials 99 (2003) 203–219.
[27] X. Ding, S. Zhou, L. Wu, G. Gu, J. Yang, Surface and Coatings Technology 205 (2010) 2554–2561.
[28] Y. Ao, J. Xu, D. Fu, C. Yuan, Applied Surface Science 255 (2008) 3137–3140.
[29] R. Kavitha, S. Meghani, V. Jayaram, Materials Science and Engineering B 139 (2007) 134–140.
[30] S. Kumar, A.G. Fedorov, J.L. Gole, Applied Catalysis B: Environmental 57 (2005) 93–107.
[31] M. Uzunova-Bujnova, R. Todorovska, D. Dimitrov, D. Todorovsky, Applied Surface Science 254 (2008) 7296–7302.
[32] B. Zhu, L. Zou, Journal of Environmental Management 90 (2009) 3217–3225.
[33] W. Zhang, Y. Li, C. Wang, P. Wang, Desalination 266 (2011) 40–45.
[34] T.P.T. Cushnie, P.K.J. Robertson, S. Officer, P.M. Pollard, R. Prabhu, C. McCullagh, J.M.C. Robertson, Journal of Photochemistry and Photobiology A: Chemistry 216 (2010) 290–294.
[35] G. Vella, G.E. Imoberdorf, A. Sclafani, A.E. Cassano, O.M. Alfano, L. Rizzuti, Applied Catalysis B: Environmental 96 (2010) 399–407.
[36] A. Danion, J. Disdier, C. Guillard, O. Paisse, N. Jaffrezic-Renault, Applied Catalysis B: Environmental 62 (2006) 274–281.
[37] H. Zhang, Y. Li, Q. Zhang, H. Wang, Materials Letters 62 (2008) 2729–2732.
[38] H.C. Liang, X.Z. Li, J. Nowotny, Solid State Phenomena 162 (2010) 295–328.
[39] F. Amano, K. Nogami, M. Tanaka, B. Ohtani, Langmuir 26 (2010) 7174–7180.
[40] N. Phonthammachai, E. Gulari, A.M. Jamieson, S. Wongkasemjit, Applied Organometallic Chemistry 20 (2006) 499–504.
[41] A. Mills, G. Hill, S. Bhopal, I. Parkin, S. O'Neill, Journal of Photochemistry and Photobiology A: Chemistry 160 (2003) 185–194.
[42] S. Malato, P. Fernández-Ibáñez, M.I. Maldonado, J. Blanco, W. Gernjak, Catalysis Today 147 (2009) 1–59.
[43] P. Robertson, I. Campbell, R. Donnacher, World Patent (2006).
[44] O.A. Salu, M. Adams, P.K.J. Robertson, L.S. Wong, C. McCullagh, Desalination and Water Treatment 26 (1–3) (2011) 87–91.
[45] C. McCullagh, N. Skillen, M. Adams, P.K.J. Robertson, Journal of Chemical Technology & Biotechnology 86 (2011) 1002–1017.